On the Microporous Nature of Mesoporous Molecular Sieves

Christine G. Göltner,*,† Bernd Smarsly, Beate Berton, and Markus Antonietti

Max-Planck Institute for Colloids and Interfaces, Research Campus Golm, 14424 Potsdam, Germany

Received May 4, 2000. Revised Manuscript Received November 30, 2000

The combination of small-angle X-ray scattering and qualitative porosimetry is applied to the puzzling phenomenon of overly large specific surface areas in some mesoporous silicas. Geometrical calculations, considering the relationship between structure, lattice parameter, and specific surface area, reveal the latter to be at least 1 order of magnitude smaller than experimental values obtained from sorption experiments, indicating the presence of micropores. Selective investigation of the mesopore system reveals that up to 63% of the specific surface area is due to microporosity. A relationship between the undirected creation of porosity and supramolecular templating is discussed.

Introduction

The introduction of nanoscale porosity into inorganic ceramic oxides is an elegant method of creating large specific surface areas, which provide a vast number of possible sorption sites for processes such as catalysis and chromatographic separation. There are two principle pathways of creating pore systems: (i) The undirected "displacement" of a porogen, either molecularly or as a result of demixing, yields a disordered arrangement of pores with a more or less broad size distribution. (ii) Templating processes allow for the synthesis of pore systems with higher degrees of order in terms of pore size distribution and structural regularity.

The overall degree of order in template-derived inorganic products depends on the template, the reaction conditions, and the mechanism of formation. For example, the synthesis of microporous crystalline zeolites is directed specifically by molecular templates, thus producing very regular pore systems with peak-shaped size distributions. It is the crystalline nature of zeolites that creates the regularity but that also represents an inherent limit to the pore diameter of 1.3 nm.[1,2]

The most versatile pathway toward larger regular inorganic pore systems is supramolecular templating. In this approach, amphiphile aggregation is utilized as a structure-directing principle for the generation of inorganics. The spontaneous self-assembly of amphiphilic molecules (surfactants or amphiphilic block copolymers) produces microphase-separated media, in whose aqueous domains inorganic sol−gel precursors can be solubilized. The solidification of the inorganic component (e.g., silica) is confined to exactly those domains and, in many cases, occurs without altering the amphiphilic aggregate structure. If this process is conducted at relatively low polymer concentrations, an organic-rich siliceous mesophase with a regular silica nanostructure precipitates.[3−10] In the presence of high template concentrations, lyotropic liquid-crystalline bulk phases are formed, which act as a supramolecular casting mold (hence the name of the procedure: nanocasting).[11−13] Nanocasting-derived siliceous ceramic oxides represent an exact cast of the lyotropic phase in which they are generated; therefore, this procedure represents one method of noninvasively replicating the aggregation structure.

Since its first mention in the literature, the process of supramolecular templating has been improved continuously, state-of-the-art being the replacement of classical surfactants by amphiphilic block copolymers (ABCs), which allow the manufacturing of thick-walled large-pore materials.[14−21] ABC templates assist in over-

* Author to whom correspondence should be addressed.
† Present address: School of Chemistry, University of Bristol, Cantock's Close, Bristol BS8 1TS, U.K.

(1) Davies, M. E.; Saldarriaga, C.; Montes, C.; Garces, J.; Crowder, C. *Nature* **1988**, *331*, 698.
(2) McCusker, L. B.; Baerlocher, C.; Jahn, A.; Bülow, M. *Zeolites* **1991**, *11*, 308.
(3) Kresge, C. T.; M Leonowicz, E.; Roth, W. J.; Vartuli, J. C.; Beck, J. S. *Nature* **1992**, *359*, 710.
(4) Vartuli, J. C.; Kresge, C. T.; Leonowicz, M. E.; Chu, A. S.; McCullen, S. B.; Johnson, I. D.; Sheppard. E. W. *Chem. Mater.* **1994**, *6*, 2070.
(5) Beck, J. S.; Vartuli, J. C.; Kennedy, G. J.; Kresge, C. T.; Roth, W. J.; Schramm, S. E. *Chem. Mater.* **1994**, *6*, 1816.
(6) Beck, J. S.; Vartuli, J. C.; Roth, W. J.; Leonowicz, M. E.; Kresge, C. T.; Schmitt, K. D.; Chu, C. T. W.; Olson, D. H.; Sheppard, E. W.; McCullen, S. B.; Higgins, J. B.; Schlenker, J. L. *J. Am. Chem. Soc.* **1992**, *114*, 10834.
(7) Monnier, A.; Schüth, F.; Huo, Q.; Kumar, D.; Margolese, D.; Maxwell, R. S.; Stucky, G. D.; Krishnamurty, M.; Petroff, P.; Firouzi, A.; Janicke, M.; Chmelka, B. F. *Science* **1993**, *261*, 1299.
(8) Huo, Q.; Margolese, D. I.; Ciesla, U.; Demuth, D. G.; Feng, P.; Gier, T. E.; Sieger, P.; Firouzi, A.; Chmelka, B. F.; Schüth, F.; Stucky, G. D. *Chem. Mater.* **1994**, *6*, 1176.
(9) Huo, Q.; Margolese, D. I.; Ciesla, U.; Feng, P.; Gier, T. E.; Sieger, P.; Leon, R.; Petroff, P. M.; Schüth, F.; Stucky, G. D. *Nature* **1994**, *368*, 317.
(10) Tanev, P. T.; Chibwe, M.; Pinnavaia, T. J. *Nature* **1994**, *368*, 321.
(11) Attard, G. S.; Glyde, J. C.; Göltner, C. G. *Nature* **1995**, *378*, 366.
(12) Attard, G. S.; Edgar, M.; Göltner, C. G. *Acta Mater.* **1998**, *46*, 751.
(13) Attard, G. S.; Göltner, C.; Corker, J. M.; Henke, S.; Templer, R. H. *Angew. Chem., Int. Ed. Engl.* **1997**, *36*, 1315.

10.1021/cm0010755 CCC: $20.00
Published on Web 04/07/2001

coming the inherent disadvantages of classical surfactants in that they introduce higher mechanical stability into the resulting hybrid material, so that under suitable reaction conditions macroscopic objects (monoliths) can be prepared.[22,23] Like their low-molecular-weight analogues, the classical surfactants, amphiphilic-block-copolymer templates can be removed by calcination.

The resulting meso- and macroporous[24] molecular sieves represent a welcome complement to classical microporous zeolites, because they can be prepared with pore diameters between 3 and 80 nm, narrow pore size distributions, and defined pore connectivities. As the result of spontaneous supramolecular self-assembly, their structures are less regular than those induced by molecular templates: Molecular templating is a consequence of specific interactions between the organic template and the inorganic precursor, thus allowing for the synthesis of single crystals of considerable size. In contrast, supramolecularly templated nanostructures reflect exactly the same density of defects (e.g., grain boundaries) that exists in the structure-directing medium.[25]

Despite their inherent defect structures, mesoporous ceramic oxides derived from the supramolecular templating of surfactants or block copolymers are often surprisingly regular. Their pore systems exhibit narrow size distributions and extraordinarily large specific surface areas. In particular, the specific surface areas of nanostructures derived from nonionic templating processes are too large to be caused exclusively by the mesopore system, which can be concluded from simple geometrical considerations. For example, a specific surface area of 1400 m^2/g was reported for mesoporous silica with hexagonally assembled cylindrical pores of 2.8-nm diameter, separated by 1.2-nm-thick walls.[11] A purely mesoporous structure, however, should have a specific surface area of 519 m^2/g, which leaves more than 60% of the surface area unaccounted for.

In theory, the surface area of template-derived porous products should be directly proportional to the overall interfacial area between the hydrophilic and hydrophobic domains in the microphase-separated medium in which the synthesis is conducted.[26] The interface area for a "two-phase" system of different geometrical structures, which is likely to be encountered for surfactant aggregates, is calculated as follows

$$\phi = \frac{8\pi}{3}\frac{R_{sph}^3}{a^3} \quad \text{for a } Im3m \text{ cubic phase } (d = 3) \quad (1)$$

$$\phi = \frac{2\pi}{\sqrt{3}}\frac{R_{cyl}^2}{a^2} \quad \text{for a hexagonal arrangement of cylinders } (d = 2) \quad (2)$$

$$\phi = \frac{2R_{lam}}{a} \quad \text{for a lamellar phase } (d = 1) \quad (3)$$

where d is the dimensionality of the structure; ϕ is the volume fraction of the hydrophobic domains (and, later, the pores); R denotes the pore radii or lamellar spacing, as appropriate (sph = sphere, cyl = cylinder, lam = lamella); and a is the periodicity (e.g., the distance between cylinders in a hexagonal phase, or the layer-to-layer or pore-to-pore distance). These equations are derived from the assumption of a geometrically perfect unit cell. The relevant distances can be determined by transmission electron microscopy (TEM). Furthermore, the interfacial area (A) per unit volume (V) is given by

$$\frac{A}{V} = d\frac{\phi}{a^2} \quad (4)$$

Finally, the specific surface area generally can be calculated by taking into account the density of noncrystalline silica (ca. 2.2 g/cm^3)[27]

$$A_{spec} = \frac{d\phi}{(1-\phi)R\rho_{SiO_2}} \quad (5)$$

Assuming hypothetical materials with a wall thickness of 3 nm and a pore radius of 2 nm (or a lamellar distance a_{lam} of 4 nm; materials of similar dimensions have been reported in the literature[19]), the hexagonal structure should have a specific surface area of around 154 m^2/g, whereas that of a cubic (bcc) structure would be 205 m^2/g and that of a lamellar one (with a lamellar distance of 4 nm and a lamellar thickness of 1 nm) would be 454 m^2/g. These calculated specific surface areas are strikingly smaller than those experimentally determined for materials with superstructures on this length scale. This difference is most probably due to microporosity, in which case the pore size distribution would be bimodal (mesoporous and microporous).

Many ceramic nanostructures are genererated in the presence of nonionic amphiphilic block copolymer templates, whose hydrophilic part is usually represented by a poly(ethylene oxide) chain. In this case, microporosity could originate from the distribution of the poly(ethylene oxide) chains throughout the whole of the aqueous/siliceous domains. Three scenarios can be envisaged for the structure of the resulting inorganic–organic hybrid material (see Figure 1): (A) The poly(ethylene oxide) blocks, albeit strongly interacting with the inorganic blocks, form a pure PEO layer at the interface with the hydrophobic block (Figure 1a) ("three-phase" system). (B) A second possibility is the homogeneous "dissolution" of the PEO chains in the aqueous

(14) Göltner, C. G.; Henke, S.; M. C. Weiβenberger, Antonietti, M. *Angew. Chem., Int. Ed. Eng.* **1998**, *37*, 613.
(15) Antonietti, M.; Berton, B.; Göltner, C.; Hentze, H.-P. *Adv. Mater.* **1998**, *10*, 154.
(16) Krämer, E.; Förster, S.; Göltner, C.; Antonietti, M. *Langmuir* **1998**, *14*, 2027.
(17) Göltner, C. G.; Berton, B.; Krämer, E.; Antonietti, M. *Chem. Commun.* **1998**, 2287–2288.
(18) Göltner, C. G.; Berton, B.; Krämer, E.; Antonietti, M. *Adv. Mater.* **1999**, *11*, 395–398.
(19) Zhao, D.; Feng, J.; Huo, Q.; Melosh, N.; Fredrickson, G. H.; Chmelka, B. F.; Stucky, G. D. *Science* **1998**, *279*, 548.
(20) Zhao, D.; Huo, Q.; Feng, J.; Chmelka, B. F.; Stucky, G. D. *J. Am. Chem. Soc.* **1998**, *120*, 6042.
(21) Zhao, D.; Yang, P.; Melosh, N.; Feng, J.; Chmelka, B. F.; Stucky, G. D. *Adv. Mater.* **1998**, *10*, 1380.
(22) Weiβenberger, M. C.; Göltner, C. G.; Antonietti, M. *Ber. Bunsen-Ges. Phys. Chem.* **1997**, *101*, 1679.
(23) Feng, P. Y.; Bu, X. H.; Stucky GD, G. D.; Pine, D. J. *J. Am. Chem. Soc.* **2000**, *122*, 994.
(24) IUPAC Manual of Symbols and Terminology. *Pure Appl. Chem.* **1972**, *31*, 578.
(25) Antonietti, M.; Göltner, C. *Angew. Chem., Int. Ed. Engl.* **1997** *36*, 910.
(26) Förster, S. Max-Planck Institute for Colloids and Interfaces, Golm, Germany, unpublished results.
(27) Groβ, S. Ph.D. Thesis, Technical University of Berlin, Berlin, Germany, 1997.

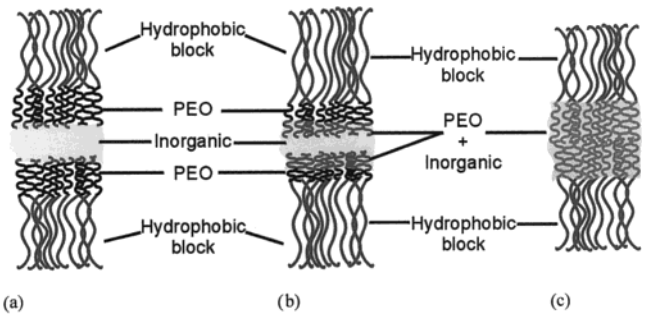

Figure 1. Three possible structures of a hybrid material composed of an inorganic phase and a nonionic amphilic block compolymer with PEO as the hydrophilic block. (a) Three-phase system (i.e., inorganic, PEO, and hydrophobic block), (b) gradual transition from a two-phase to a three-phase system, and (c) two-phase system (PEO/inorganic and hydrophobic block).

solution of the inorganic precursor, which results in a "two-phase" system (Figure 1c). In addition to the supramolecular template, each hydrated ethylene oxide chain acts as a nonspecific template in its own right. The templating procedure in a two-phase system can therefore be called hierarchical. (C) Another case would be a gradual transition from a two-phase to a three-phase system, where the poly(ethylene oxide) chains are dissolved in the inorganic phase, but a saturation limit dictates the beginning of microphase separation. In this transition, a certain degree of microporosity and a simultaneous increase in the mesopore diameter are to be expected (Figure 1b).

NMR spectroscopic investigations of regularly structured hybrid materials consisting of amphiphilic block copolymer and sol−gel-derived aluminosilicate have shown that there is no obvious dynamic heterogeneity in the poly(ethylene oxide) chains.[28] Wiesner et al. reported that the hydrophilic blocks are firmly anchored in the inorganic blocks, giving rise to substantial restriction of the molecular mobility, whereas the hydrophobic blocks of the template show a flexibility comparable to that observed for the bulk copolymer. These studies suggest a homogeneous distribution of the ethylene oxide chains within the inorganic matrix, which will cause considerable microporosity (Figure 1a).

The true nature of a pore system is an important feature whenever applications sensitive to pore size and geometry are concerned. It is therefore the aim of this paper to elucidate the pore sizes and pore size distributions of mesoporous inorganic nanostructures. Two different complementary methods are applied to characterize the true nature of the pore system.

First, nitrogen sorption experiments are used to estimate the specific surface areas as well as the sizes and volumes of the pore systems. Within the scope of this technique, selective investigation of the mesopore system is possible by filling the micropores with an adsorbent less volatile than nitrogen (blocking of micropores). Porosimetry measurements of blocked and redesorbed samples reveal the mesopore surface area as well as the pore volumes. The micropore characteristics are then accessible by subtraction of the sorption curves of blocked and unblocked materials.

In addition, the occurrence of microporosity is independently investigated and characterized by a novel method of evaluating the data obtained from small-angle X-ray scattering (SAXS) experiments.[29] This new approach is based on the previously established[30−32] so-called "chord-length distribution" (CLD), obtained by fitting the whole range of the SAXS curve with orthogonal functions, which are then analytically Fourier transformed. Simplistically, the chord-length distribution is a quantitative measure for the distances between phase boundaries (the only structural element that scatters X-rays, assuming a continuous medium) in dense, multiphase systems. Relevant material information, such as the average pore size, pore geometry, and prevalent length scales, is thus obtained from a noninvasive SAXS experiment, which is especially useful for weakly ordered or unordered (i.e., nonzeolitic) materials. The mean chord length l_p, or the so-called Porod length, is obtained by averaging the CLD and is directly related to the ratio of specific surface to volume A/V via eq 6

$$l_p = 4\phi(1-\phi)\frac{V}{A} \tag{6}$$

where ϕ is the volume fraction of one of the two phases. Compared with conventional algorithms, the numerical evaluation of the CLD from SAXS data is numerically very stable and therefore reliable. Quantitative structural parameters are obtained with a reasonable error estimation, which is crucial, especially for the quantification of microporosity.

Both nitrogen sorption and SAXS experiments were applied to mesoporous silicas derived by nanocasting of lyotropic amphiphilic block copolymers templates. The templates used were commercially available block copolymers consisting of a hydrophobic polystyrene block and a hydrophilic poly(ethylene oxide) block (so-called SE$m/n$ s, where m = molar mass of hydrophobic block/100 and n = molar mass of hydrophilic block/100, see Table 1). The structures of these SE-templated silicas, which have been reported previously,[14] do not represent any of those known for conventional lyotropic surfactant or ABC bulk phases, but the materials show hexagonal symmetry (as assessed by small-angle X-ray diffraction, SAXS), narrow pore size distributions and even wall thicknesses, and they are bicontinuous. The materials are formed and used as large particles in order to avoid significant surface area contributions from outer particle surfaces.

The experiments presented here are not only valid for the systems under investigation but are also expected to allow for generalization toward an analysis of all mesoporous ceramics created by templated assemblies of nonionic surfactants.

Experimental Section

Instruments. TEM micrographs were obtained with a Zeiss EM 912 OMEGA instrument operating at an acceleration voltage of 120 kV. Samples were ground and suspended in acetone. One droplet of the suspension was applied to a carbon-coated 400-mesh copper grid and left to dry. Nitrogen sorption

(28) De Paul, S. M.; Zwanziger, J. W.; Ulrich, R.; Wiesner, U.; Spiess, H. W. *J. Am. Chem. Soc.* **1999**, *121*, 5727.

(29) Smarsly, B.; Burger, C., to be published.
(30) Méring, J.; Tchoubar, D. *J. Appl. Crystallogr.* **1968**, *1*, 153.
(31) Perret, R.; Ruland, W. *J. Appl. Crystallogr.* **1970**, *3*, 525.
(32) Torquato, S.; Lu, B. *Phys. Rev. E* **1993**, *47*, 2950.

Table 1. Composition of Templates Used for Nanocasting

template name	M_w of polystyrene block (kg/mol)	M_w of poly(ethylene oxide) block (kg/mol)
SE10/10	1	1
SE30/30	3	3
SE10/50	1	5
PEO20	0	2
PEO100	0	10

experiments were conducted using a Micromeritics Gemini instrument. Samples were degassed at 100 °C in vacuo for 12 h prior to investigation.

Small-angle X-ray scattering measurements were carried out with a Nonius rotating anode ($P = 4$ kW, $\lambda = 0.154$ nm) using image plates. With the image plates placed at a distance of 40 cm from the sample, a scattering vector range of $s = 0.07-1.6$ nm^{-1} was available. After being heated to 300 °C for 5 h, the samples were irradiated for 10 h to obtain satisfying scattering statistics. 2D diffraction patterns were transformed into 1D radial averages. The data noise was calculated according to Poisson statistics, which is a valid approach for scattering experiments.

Materials and Methods. Amphiphilic block copolymers of the SE type were kindly provided by Th. Goldschmidt AG, Essen, Germany, and used without further purification. Poly(ethylene oxide) ($M_w = 2$ and 10 kg/mol) (Fluka), TMOS, and *n*-nonane (Aldrich) were used as received. For the synthesis of porous silicas, the porogen (template) was dissolved in TMOS with slight heating. After the mixture was cooled to room temperature, hydrochloric acid (pH 2) was added, upon which exothermal hydrolysis of TMOS occurred. After this reaction had abated, the mixture was evacuated on a rotary evaporator (water bath of 40 °C) for 10 min. The resulting clear viscous fluid was placed in a drying oven (60 °C, ambient pressure) overnight for solidification. To remove the organic matter from the solid hybrid materials, the products were calcined at 500 °C (12 h with nitrogen, 12 h with oxygen). The templates used for the synthesis of mesoporous silicas presented in this paper are listed in Table 1.

Results and Discussion

Four types of silicas were investigated in order to allow the quantitative description of the pore systems: (i) Silicas made in the presence of SE-block copolymers with constant block length ratios but different molecular weight (SE10/10 and SE30/30) were used to demonstrate the dependence of the mesopore diameter on the volume of the hydrophobic block. These templates were applied at constant mass ratios ABC/silica. (ii) Silicas templated with SE-block copolymers of varying block-length ratios (SE10/10 and SE10/50) and constant hydrophobic block lengths were templated under conditions such that the polystyrene/silica volume ratio was kept constant. (iii) A mixture of SE10/10 and poly(ethylene oxide) was templated to determine whether the combination of supramolecular template and nondirecting porogen has the same effect on the sorption properties as a similar increase in the amount of PEO bound to the block copolymer mentioned in ii. (iv) Porous silicas made in the presence of different amounts of poly(ethylene oxide) homopolymers were used for the elucidation of nanoscale amorphous microporosity. The molecular-weight dependence of the pore structures for these porogens was also studied.

To determine whether the synthesis or calcination process induces porosity, a sol−gel silica was prepared similarly to all of the other samples except that no organic porogen was added. It this case, both nitrogen sorption experiments and SAXS measurements revealed a negligible specific surface area.

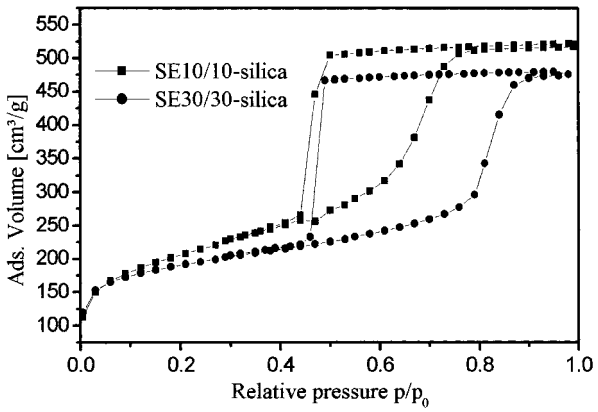

Figure 2. Nitrogen sorption isotherms of SE10/10- (■) and SE30/30-silica (●).

All silicas made in the presence of amphiphilic molecules, however, had the desired pore structure. Nitrogen sorption experiments of SE10/10-templated silica as a representative example (its adsorption−desorption isotherm is shown in Figure 2) indicate a BET surface area of 710 m^2/g.

The steep slope at low relative pressures in the sorption curve suggests that the isotherm is not strictly of type IV, but that it represents a superposition of type I and type IV isotherms, indicating the presence of micropores. Microporosity seems to be a substantial contributor to the specific surface area, as an interface (and later mesopore surface area) of ca. 140 m^2/g is expected on the basis of geometrical calculations.[33] Nitrogen sorption experiments, however, reveal the specific surface area to be substantially higher. The sorption isotherm of the SE30/30-templated analogue shows the same qualitative features, with the difference that pore condensation and its hysteresis occur at higher relative pressures, which is expected for this material because its pores are substantially larger than those of SE10/10-silica. As shown previously by TEM and sorption experiments,[14] the pore diameter correlates with the size of the hydrophobic block of the template. The specific surface area in this sample, as indicated by nitrogen sorption experiments, is 620 m^2/g, which again is higher than expected from a strictly mesoporous material with the dimensions found previously.[14] In addition, the isotherm shows an extraordinarily high *C* value of 900, which represents a strong indicator for the existence of micropores. A so-called *t*-plot analysis was also attempted to elucidate the structure of the pore system. A *t* plot is the plot of the adsorbed layer thickness versus volume adsorbed. Extrapolation of the straight line observed in this graphical representation (not shown here) toward the *y* axis allows for the determination of the external surface area, and subtraction of this value from the overall surface area provides a value of the micropore area. However, this method does not appear to be suitable for the systems under investigation, as a graphical extrapolation of the *t* plot provides a value for the layer thickness that is larger than

(33) Berton, B. Ph.D. Thesis, University of Potsdam, Potsdam, Germany, 1999.

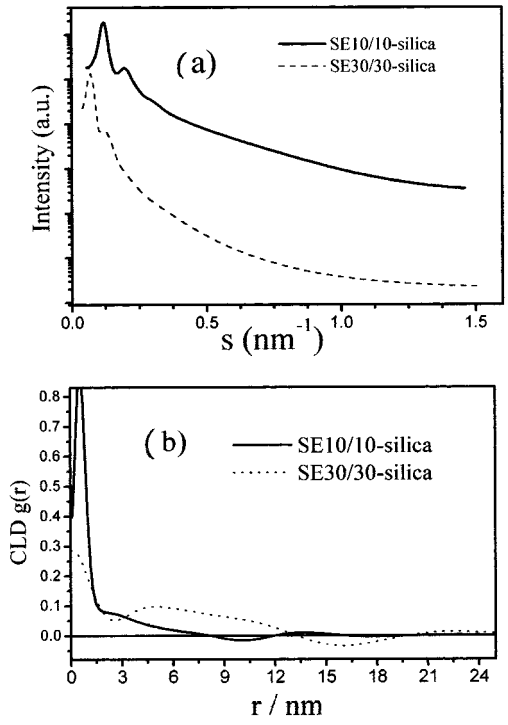

Figure 3. (a) SAXS curves of SE10/10- and SE30/30-silica, (b) chord-length distributions $g(r)$ of SE10/10- and SE30/30-silica. The large contributions at small r reflect the existence of micropores. The different shapes of the CLD functions at small r indicate the differences in the degree of microporosity.

the actual pore diameter, which did not make sense, and therefore, this approach was not pursued any further.

The existence of micropores in SE10/10-silica, however, is confirmed by the SAXS data (the scattering curves are shown in Figure 3a), which agree well with the sorption experiments.

The specific surface areas are evaluated to be 750 ± 50 m^2/g for SE10/10-silica and 610 ± 30 m^2/g for SE30/30-silica. These values are calculated from l_p according to eq 6 assuming a volume fraction of pores of 0.6, as was determined from the nitrogen sorption data. The error inherent in the result is essentially due to this estimation, the error in the determination of l_p is much smaller. However, it was regarded as more appropriate to rely on estimated values for the volume fraction rather than on those obtained from porosimetry data in order to provide two independent data sets, one from X-ray evaluation and one from sorption studies. The values for the specific surface areas correlate well with the nitrogen sorption analysis, indicating complete accessibility of the pores for gaseous nitrogen. However, the values of the mean chord length (l_p = 1.25 ± 0.08 nm for SE10/10-silica and l_p = 2.00 ± 0.05 nm for SE30/30-silica), which is a measure for the average pore size, are well below the values expected for a purely mesoporous material with a structure as observed by TEM. This is just another indication that microporosity significantly contributes to the surface characteristics of the templated materials.

A detailed analysis of the CLD function (see Figure 3b) allows for a separate estimation of the average micro- and mesopore diameters and also the wall thickness. In simple terms, the first maxima can be directly related to the size of the different types of pores and also of the walls, whereas the first minimum in the curve is a measure of the periodicity of the structure. The CLD functions of the two materials reveal a bimodal pore size distribution, with 0.8−1.5-nm-sized micropores in both SE10/10- and SE30/30-silica and 5.5- and 8.5-nm mesopores in SE10/10-silica and SE30/30-silica, respectively. The mean micropore diameter was determined by a separate analysis of the behavior of the CLDs at small r below 2.5 nm. The micropores show a broad size distribution between 0.8 and 1.5 nm. Although in many cases the determination of pore sizes from CLDs is complex because of the superposition of the chords of "walls" and "pores", from TEM analysis, the maxima and the subsequent shoulders at ca. 3 (SE10/10-silica) and 5.5 nm (SE30/30-silica) can be attributed to the walls. The periodicities are obtained as 8.3 (SE10/10) and 14.0 nm (SE30/30) from the interference peaks in the SAXS patterns, the difference between the values being the mean mesopore diameter. These conclusions are supported by a recent investigation of nitrogen sorption in SE-silicas by in situ small-angle neutron scattering.[34] Judging from volume considerations, it is evident that such thick walls can only be made (within the used recipe) if the walls are (micro)-porous in their own right. Based on the fact that the surface area is bound to decrease with increasing pore size, it is not surprising to find a smaller surface area for SE30/30 silica as compared with its SE10/10-derived analogue, regardless of the analytical method applied.

To investigate the effect of the hydrophilic block on the overall porosity of the silica nanostructures, samples were prepared in the presence of a template with a significantly higher molecular weight of the hydrophilic block (SE10/50), with the length and absolute amount of hydrophobic units kept constant. A comparison of the sorption data obtained for SE10/10-silica with those of SE10/50-silica reveals an increase in the specific surface area (see Table 2) from 710 to 785 m^2/g.

At the same time, the mesopore diameter, as determined from the desorption branches of the nitrogen sorption isotherm (BJH method) as well as the TEM images (Figure 4), increases substantially from 4.2 (SE10/10-silica) to 5.4 nm (SE10/50-silica). The mesopore diameter, therefore, can not be attributed to the hydrophobic moieties of the template only but must also contain contributions that are related to the hydrophilic PEO in the sol−gel system. The substantial increase in the specific surface area from SE10/10-silica to SE10/50-silica with increasing in the mesopore diameter is attributed to the presence of additional micropores. Increasing the molecular weight of PEO covalently attached to the hydrophobic core, therefore, increases both the mesopore size and the microporosity.

The evaluation of the SAXS data reveals the same trends: the mean chord length of SE10/50-silica (1.08 nm) is significantly smaller than that of SE10/10-silica (1.25 nm), which is essentially due to additional microporosity. The related specific surface area, as obtained from the evaluation of the SAXS data, increases from 750 (SE10/10-silica) to 840 m^2/g (SE10/50-silica) and confirms the results of the nitrogen sorption experiments. Detailed analysis of the chord-length distribu-

(34) Smarsly, B.; Göltner, C.; Antonietti, M.; Ruland, W.; Hoinkis, E. *J. Phys. Chem. B* **2001**, *105*, 831.

Table 2. Recipes for Porous Silicas

name	template (g)	PEO (g)	HCl (pH 2) (g)	TMOS (g)	mean chord length l_p (nm)	BET surface area (m^2/g)	pore diameter (TEM) (nm)	pore diameter (BJH)[d] (nm)
SE10/10-silica[a]	2.0	−	2.0	4.0	1.25 ± 0.08	710	4.2	3.8
SE10/50-silica[a]	4.0	−	4.0	8.0	1.08 ± 0.06	785	5.4	2.3
SE30/30-silica[a]	2.0	−	2.0	4.0	2.00 ± 0.05	610	8.5	7.1
PEO20-silica[b]	−	2.0	2.0	4.0	1.40 ± 0.06	951	NA	NA
PEO100-silica[b]	−	2.0	2.0	4.0	1.45 ± 0.07	907	NA	NA
PEO100-silica 11[b]	−	0.5	2.0	4.0	−	230	NA	NA
PEO100-silica 20[b]	−	1.0	2.0	4.0	0.70 ± 0.04	540	NA	NA
PEO100-silica 27[b]	−	1.5	2.0	4.0	0.80 ± 0.05	630	NA	2.5
PEO100-silica 33[b]	−	2.0	2.0	4.0	1.45 ± 0.07	900	NA	2.8
PEO100-silica 43[b]	−	3.0	2.0	4.0	1.65 ± 0.10	880	NA	4.2
PEO100-silica 50[b]	−	4.0	2.0	4.0	−	770	NA	5.1
SE-PEO(10)-silica[a,c]	2.0	0.4	2.0	4.0	−	922	NA	3.7
SE-PEO(20)-silica[a,c]	2.0	0.8	2.0	4.0	−	983	NA	3.7
SE-PEO(30)-silica[a,c]	2.0	1.2	22.0	4.0	−	908	NA	3.7

[a] Supramolecular templating. [b] Undirected displacement of porogen. [c] Numbers in parentheses represent the weight percentage of PEO-20 with respect to template. [d] Determined from the desorption branch of the isotherm.

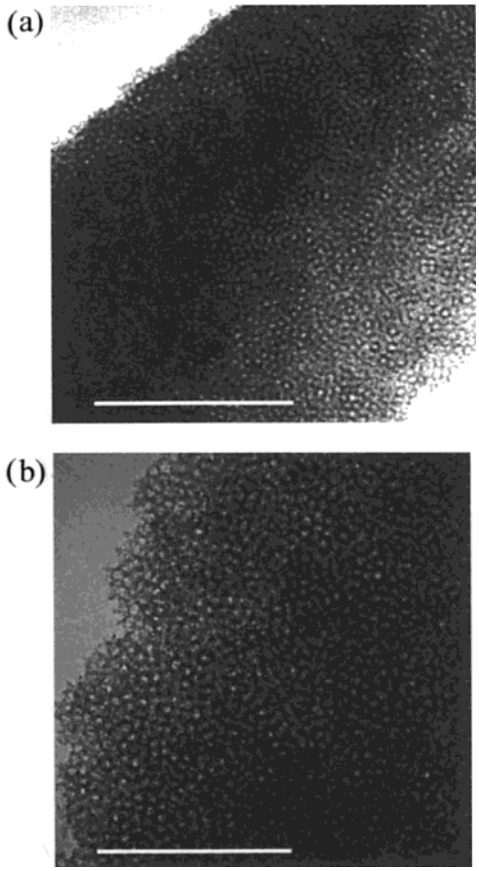

Figure 4. TEM images of (a) SE10/10- and (b) SE10/50-silica. Scale bar corresponds to 200 nm.

tions of SE10/50-silica indeed shows an increase in the mean diameter of mesopores as compared to those of SE10/10-silica, as well as a significant increase in the peak height due to the micropores, which is in agreement with the results of the sorption experiments and TEM studies.

Further evidence for the origin of the additional microporosity in mesoporous silicas is obtained by investigating a series of samples prepared in the presence of mixed templates consisting of the self-organizing SE10/10 and differing amounts of PEO homopolymer that are not covalently bound to the ordered structure. TEM analyses of those materials reveal only minor qualitative structural differences in the mesopore system of these silicas. The samples appear less ordered than the corresponding ones prepared with pure SE templates. This loss of order is attributed to osmotic disturbances in the intermolecular potentials between the SE assemblies caused by the presence of the linear PEO chains, which, however, does not result in local structure changes, but in long-range order effects only. The mesopore diameter of the PEO-containing samples increases with increasing PEO contents, which agrees well with the results discussed above. It is assumed that some of the PEO (either from block copolymer or from homopolymer) contributes to the mesopore radius, presumably by demixing from the solidifying matrix at higher PEO concentrations. It is interesting to note that hydrophilic PEO, albeit miscible with the siliceous aqueous phase and usually repelled from the block copolymer aggregates, contributes to the mesopore diameter, i.e., the interpretation of thermodynamic demixing of PEO and a glassy matrix is supported. The specific surface areas of these samples are listed in Table 2. The surface area first increases with increasing PEO homopolymer content, but it then seems to level out and reach a limiting value. This fact is attributed to the limited solubility of PEO in silica. Nitrogen sorption experiments produce the expected isotherms consisting of a superposition of type I and type IV.

If the microporosity observed for SE-templated silica is caused by the poly(ethylene oxide) chains being molecularly distributed in the silica matrix during the sol−gel process, a purely microporous material is expected from the sol−gel synthesis of silica in the presence of ethylene oxide homopolymers. The synthesis of PEO-silica represents the displacement of the sol−gel precursor by individual dissolved polymer chains rather than supramolecular templates. Indeed, silicas obtained in the presence of poly(ethylene oxide) do not show any degree of order, as revealed by X-ray diffraction and TEM analysis. Furthermore, no mesoporosity is evidenced by TEM (not shown), although a small-scale contrast variation indicates the presence of structural elements below the limit of satisfactory resolution.

PEO20- and PEO100-silicas were prepared with the same amounts of poly(ethylene oxide) that is present in the synthesis of SE10/10-silica (Table 2). Nitrogen sorption experiments reveal type I isotherms, which are indicative of microporous materials. The unexpected occurrence of a small hysteresis loop (the adsorption−

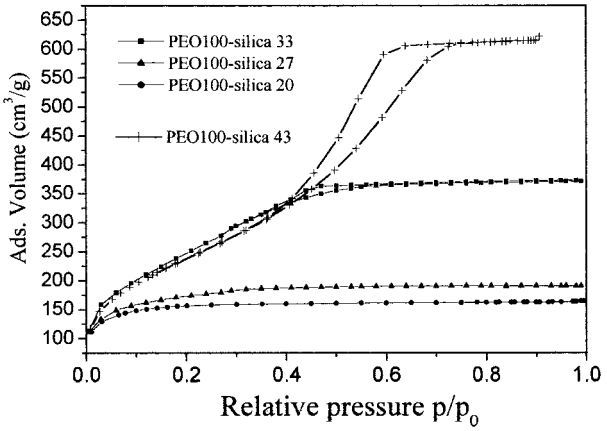

Figure 5. Nitrogen sorption isotherms of PEO100-silicas generated in the presence of different amounts of PEO.

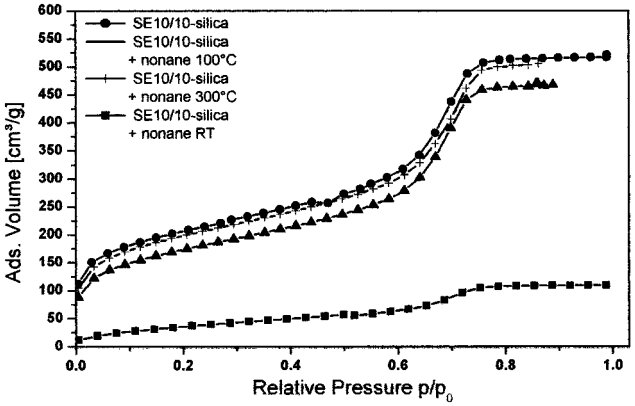

Figure 6. Nitrogen adsorption isotherms of SE10/10 silica and of SE10/10-silica after the micropores are blocked with *n*-nonane. The sorption data show that micropores are preferentially filled while mesopores remain accessible.

desorption isotherm of PEO100-silica as a representative example is shown in Figure 5, squares), however, gives rise to the assumption that the material also exhibits a certain degree of mesoporosity. The specific surface areas of PEO-"templated" silicas are around 920 m^2/g.

The conclusions drawn from the sorption characteristics are confirmed by the evaluation of the SAXS data. Here also, an unexpected structural similarity of these microporous silicas is revealed. The CLDs of PEO20- and PEO100-silica are found to be identical within the limit of error with mean chord lengths of $l_p = 1.40 \pm 0.06$ (PEO20-silica) and 1.45 ± 0.07 nm (PEO100-silica). Obviously, variations of the molar mass have no significant influence on the pore structure and pore sizes, which agrees well with the expectation that PEO is molecularly dissolved within the sol−gel system.

The pore size of silicas prepared in the presence of PEO depends on the amount of PEO in the sol−gel mixture. Experiments employing lower amounts of PEO yield materials whose specific surface areas and mean pore diameters (as revealed by X-ray diffraction studies) are smaller than those for samples generated in the presence of larger porogen contents. A mean chord length of $l_p = 0.7 \pm 0.04$ nm indicates the smaller dimensions of the porous system compared with those of the materials made with higher PEO contents. The pore size distribution curves calculated from the SAXS data for all of the PEO-silicas show the same maximum corresponding to a pore diameter of 0.5 nm. This value corresponds well with the cross section of a single stretched, hydrated poly(ethylene oxide) chain.

Whereas samples prepared in the presence of small amounts of PEO-20 as the porogen show only one maximum in the CLD, the curves of materials made at higher PEO concentration show something reminiscent of a bimodal pore size distribution. This phenomenon can be explained by the fact that, with increasing PEO concentration, the likelihood of templating "chain pairs" increases, i.e., two PEO chains form the pore. The probability of PEO chains occurring in close vicinity to each other and the probability of intersects between PEO chains increase with the square of the concentration. With increasing PEO contents, the number of "molecularly generated pores" (micropores caused by one single PEO chain) increases with the PEO content until the occurrence of pairs or strands becomes likely. It is this saturation concentration above which mesoporosity is observed in addition to microporosity. This point is determined by comparing the SAXS and sorption data of various silica samples prepared in the presence of different amounts of PEO as the porogen. At lower PEO contents, the pore diameter remains constant (SAXS), while the specific surface area increases linearly with the amount of PEO in the sol−gel mixture. At a concentration similar to that present during the templating of SE10/10 and SE10/50, PEO begins to cause additional mesoporosity (Table 2). A distinct onset of demixing, as found for the SE templates, was not observed for the pure PEO templates, which is presumably due to the fact that the concentration steps for the homopolymers can be increased more gradually than those in the blockcopolymer, which are only available with a certain molecular weight.

Finally, the mesopore system of SE10/10-silica was qualitatively elucidated by selectively blocking the micropores with nonane. The nitrogen adsorption isotherms are shown in Figure 6. This figure clearly shows that the mesopore system can be individually detected by preventing the adsorption of nitrogen in the micropores. These results are another independent indication of microporosity in nanocasting-derived mesoporous silicas.

Conclusions and Outlook

The results presented in this paper provide deeper insight into the real nature of pore systems derived either by nanocasting of nonionic amphiphilic block copolymers and surfactants or by the undirected displacement of a nonaggregating porogen (e.g., solvating polymer chains). The combination of simple nitrogen sorption results with the detailed evaluation of scattering data allows for a quantitative description of the pore systems with respect to size and surface area. It was shown that the micropores in the mesoporous inorganic nanostructures are generated by the water- and silica-compatible PEO chains, which, at low PEO concentrations, create pores of a size comparable to the diameter of a hydrated PEO chain. At higher PEO concentrations, as observed locally for most assemblies of nonionic amphiphiles, PEO contributes to both the meso- and micropores, which suggests an underlying three-phase

structure, similar to that shown in Figure 1b. It is interesting to note that a type of "condensation" or demixing of PEO chains onto the hydrophobic cores is found for the supramolecular templates. In contrast, the casts of pure PEO solutions show mesoporosity that is due only to the multiple PEO structures, that is, strands of PEO chains that exist for purely statistical reasons as a function of high PEO concentration.

Judging from the specific surface areas alone, a substantial amount of microporosity can be assumed to be present in most inorganic nanostructures derived from supramolecular templating of nonionic surfactants and block copolymers. This conclusion represents a serious restriction for all effects that rely on size-specific "vectorial" or symmetry-related sorption processes as well as for the mechanical performance of the porous frameworks, but it might also open access to new hierarchically structured pore systems. The combination of the simple analytical techniques presented here can be utilized as a tool to develop synthetic strategies toward purely mesoporous structures or to design the pore sizes in materials with multimodal pore size distributions.

Acknowledgment. The authors thank E. Krämer for preparative assistance, C. Burger for helpful discussions, Th. Goldschmidt AG, Essen (Germany), for the generous supply of SE block copolymers, and the Max-Planck Gesellschaft for financial support.

CM0010755